BBA - Molecular Basis of Disease 1865 (2019) 1421–1427

Contents lists available at ScienceDirect

BBA - Molecular Basis of Disease

journal homepage: www.elsevier.com/locate/bbadis

Long non-coding RNA cytoskeleton regulator RNA (CYTOR) modulates pathological cardiac hypertrophy through miR-155-mediated IKKi signaling

Yuan Yuan[a,1], Juan Wang[b,1], Qiuxiang Chen[c,d], Qingqing Wu[a], Wei Deng[a], Heng Zhou[a], Difei Shen[a,b,d,*]

[a] Department of Cardiology, Renmin Hospital of Wuhan University, Cardiovascular Research Institute of Wuhan University, Hubei Key Laboratory of Cardiology, Wuhan 430060, China
[b] Department of Cardiology, The Fifth Affiliated Hospital of Xin Jiang Medical University, Urumchi 830001, China
[c] Department of Neurology, Renmin Hospital of Wuhan University, Wuhan 430060, China
[d] Qianjiang Central Hospital of Hubei Province, Qianjiang 433100, China

ARTICLE INFO

Keywords:
Cardiac hypertrophy
lncRNA CYTOR
miR-155
IKBKE
NF-κB signaling

ABSTRACT

Pathological cardiac hypertrophy, which may lead to heart failure and sudden death, can be affected by multiple factors. In our previous study, we revealed that IKKi deficiency induced cardiac hypertrophy through the activation of the AKT and NF-kB signaling pathway in response to aortic banding (AB). Non-coding RNAs, mainly long non-coding RNAs (lncRNAs) and microRNAs (miRNAs), play a crucial role in normal developmental and pathological processes. In the present study, microarray analysis results from GEO database were analyzed, and upregulated lncRNAs in cardiac hypertrophy were identified. Of them, lncRNA cytoskeleton regulator RNA (CYTOR) obtained a fold-change of 6.16 and was positively correlated with IKBKE according to the data from The GTEx project. CYTOR knockdown significantly enhanced the inducible effect of AB operation on mice myocardial hypertrophy and Angiotensin II on cardiomyocyte hypertrophy. Moreover, miR-155 was significantly related to hypertrophic cardiomyopathy (HCM, |hsa05410) and predicted to target both CYTOR and IKBKE. Luciferase reporter and RIP assays revealed that CYTOR served as a ceRNA for miR-155 to counteract miR-155-mediated repression of IKBKE. Moreover, CYTOR knockdown reduced IKKi protein levels while activated NF-kB signaling pathway, whereas miR-155 inhibition exerted an opposing effect; the effect of CYTOR could be partially attenuated by miR-155 inhibition. Taken together, CYTOR might play a protective role in cardiac hypertrophy through miR-155 and downstream IKKi and NF-κB signaling, most possibly through serving as a ceRNA for miR-155 to counteract miR-155-mediated repression of IKBKE.

1. Introduction

Pathological cardiac hypertrophy, one of the most critical risk factors for the progression of heart failure, can be attributed to long-term hypertrophic stress, such as hypertension, ischemia, myocarditis, and valvular disease [1,2]. Under normal physiological conditions, cardiac hypertrophy maintains heart function efficiently. However, persistent hypertrophy causes the deposition of extracellular collagen, the loss of adrenergic responsivity, and metabolic changes [3]. Together, these alterations result in cell apoptosis and irreversible cardiac structural remodeling, which ultimately leads to heart failure and sudden death [3–5].

Numerous studies have demonstrated various specific peptide hormones, growth factors, and cytokines with cardioprotective function. Phosphoinositide 3-kinase (PI3K) and its downstream serine-threonine kinase, AKT (or Protein Kinase B) exerts cardioprotective effects in cardiac hypertrophy models [4,6]. Our previous study identified that the loss of inducible IkB kinase (IKKi/IKKe), a recently reported serine-threonine IKK-related kinase, which could activate AKT independent of PI3K [7], aggravated aortic banding-induced cardiac hypertrophy through activating the AKT and NF-κB signaling pathways [8]. In cultured cells, IKKi overexpression also suppressed the AKT and NF-kB signaling pathways [6]. Developing a deeper understanding of the regulation of IKKi signaling may provide novel strategies for the treatment of pathological cardiac hypertrophy and heart failure.

Of the mammalian genome, protein-coding genes take up about

* Corresponding author at: Department of Cardiology, Renmin Hospital of Wuhan University, Cardiovascular Research Institute of Wuhan University, Hubei Key Laboratory of Cardiology, Wuhan 430060, China.
E-mail address: rm000137@whu.edu.cn (D. Shen).
[1] The authors contributed equally to this manuscript.

https://doi.org/10.1016/j.bbadis.2019.02.014
Received 22 August 2018; Received in revised form 13 February 2019; Accepted 14 February 2019
Available online 19 February 2019
0925-4439/

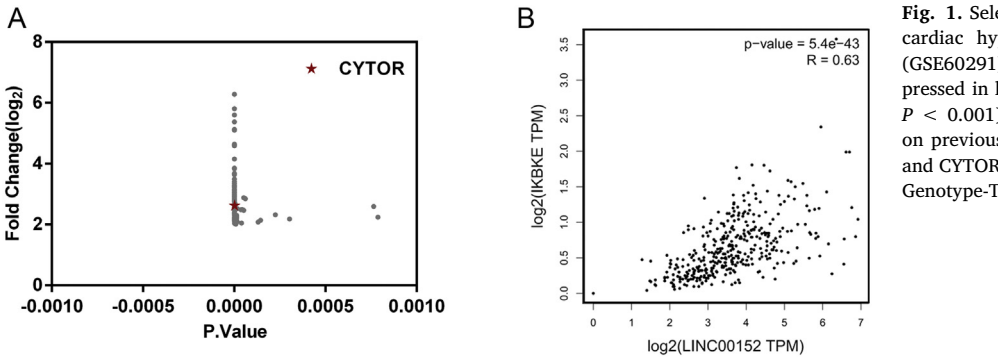

Fig. 1. Selection of differentially-expressed lncRNAs in cardiac hypertrophy (A) According to GEO database (GSE60291), a total of 187 lncRNAs were highly expressed in human cardiac hypertrophy (fold-change > 4, $P < 0.001$). Of them, lncRNA CYTOR was selected based on previous studies. (B) The correlation between IKBKE and CYTOR expression was analyzed using data from The Genotype-Tissue Expression (GTEx) project.

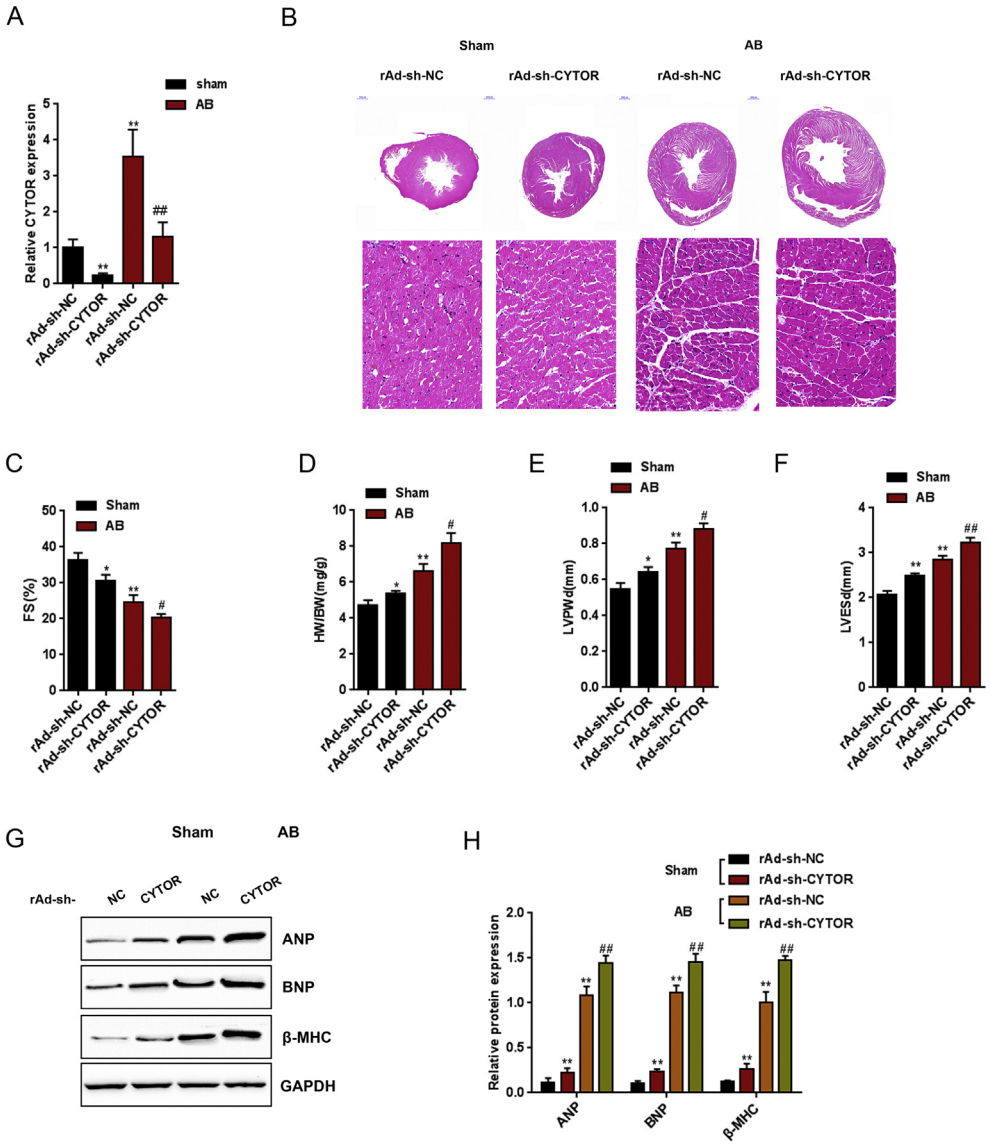

Fig. 2. The effect of CYTOR knockdown on cardiac hypertrophy (A) CYTOR expression in mice hearts from the indicated groups was examined using real-time PCR. (B) The cellular morphology of sham-operation and AB-operation mice (wild-type and CYTOR knockdown) was examined using H&E staining. (C–F) Anatomic and echocardiographic analysis. (G–H) The protein levels of ANP, BNP and β-MHC were examined using Immunoblotting. The data are presented as mean ± SD of three independent experiments. $*P < 0.05$, $**P < 0.01$, *vs.* rAd-sh-NC-infected mice in Sham group; $\#P < 0.05$, $\#\#P < 0.01$, *vs.* rAd-sh-NC-infected mice in AB group.

1.5%, while non-coding RNAs (ncRNAs) account for more substantial genomic parts [9]. The ncRNAs have a beneficial effect in sustaining the normal physiological functions of cells [10–12]. Long non-coding RNAs (lncRNAs) and microRNAs (miRNAs) both are a crucial constituent part of ncRNAs. Numerous miRNAs have been indicated to affect heart hypertrophy, such as miR-1, miR-133, and miR-214 [13–15]. In addition, lncRNAs have been reported play critical regulatory roles in cardiovascular disease, particularly in heart hypertrophy [16–20]. Regarding the molecular mechanism, the competitive endogenous RNAs (ceRNA), containing shared microRNA response elements (MREs),

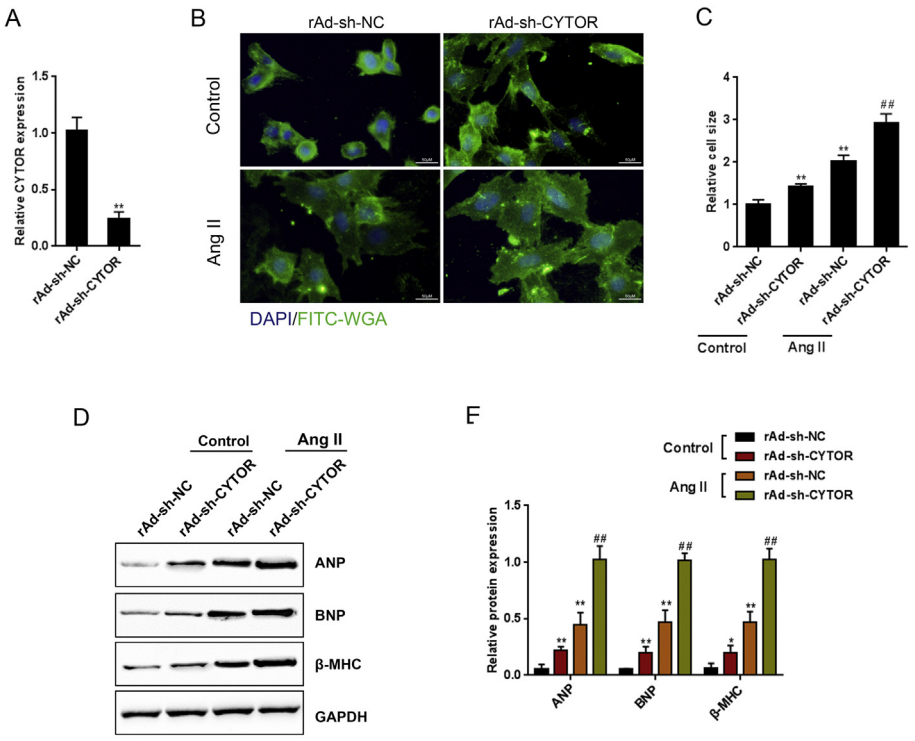

Fig. 3. CYTOR knockdown aggravates Ang II-induced cardiomyocyte hypertrophy *in vitro* (A) The promotive effect of CYTOR knockdown on the enlargement of myocyte induced by Ang II (1 μM for 48 h). (B) The relative cell size was analyzed. (C–D) The protein levels of ANP, BNP and β-MHC in sh-CYTOR infected myocytes in the presence or absence of Ang II treatment. The data are presented as mean ± SD of three independent experiments. $*P < 0.05$, $**P < 0.01$, *vs.* r Ad-sh-NC-infected myocytes in control group; $\#P < 0.05$, $\#\#P < 0.01$, *vs.* rAd-sh-NC-infected myocytes in Ang II treatment group.

could bind to microRNA efficiently. Therefore, the existence of ceRNA will affect the activity of microRNAs [21]. Salmena et al. speculated that these ceRNAs, including protein-coding genes, pseudogenes, and long non-coding RNAs, could interact with each other to form a ceRNA network with their ability of binding to microRNA [22]. The communication forms extensive cis and trans-regulatory crosstalk throughout the transcriptome. However, how the ceRNA network participates in the progression of cardiac hypertrophy needs further elucidation.

During the present exploration, based on GEO database (GSE60291), we identified dysregulated lncRNAs in human cardiac hypertrophy and selected lncRNA cytoskeleton regulator RNA (CYTOR) due to its high expression and positive correlation with IKBKE. Next, the detailed functions of CYTOR knockdown on heart hypertrophy *in vivo* and *in vitro* were examined. By performing KEGG and Mirpath annotation, miRNAs related to hypertrophic cardiomyopathy (HCM, |hsa05410) were identified, and miR-155 was selected because of its role in hypertrophic cardiomyopathy [23]. The predicted interactions of CYTOR, miR-155 and IKBKE were validated, and the dynamic effect of CYTOR/miR-155 axis on hypertrophic cardiomyopathy and downstream IKKi and NF-κB signaling pathway was illustrated.

2. Materials and methods

2.1. Animals and animal models

All animal procedures were performed in accordance with the Guide for the Care and Use of Laboratory Animals, which was published by the U.S. National Institutes of Health (NIH Publication No. 85-23, revised 1996) and approved by the Animal Care and Use Committee of the Renmin Hospital of Wuhan University. Male SD rats were purchased from experimental animal center of Wuhan University. A renovascular hypertensive model was induced by the aortic banding (AB) method for 4 weeks according to previous reports [24]. Adenovirus with shCYTOR (CYTOR in rat named LOC100910286) or sh-NC (rAd-sh-CYTOR, rAd-sh-NC) were purchased from Genechem, Co. Ltd., China (the viral titer is 1×10^{10} PFU/mL). 100 μL of adenovirus were injected through tail vein 3 weeks before the further experiment.

Echocardiography was performed as described previously [8]. The left ventricle (LV) dimensions were measured in the parasternal short-axis view. The left ventricular end systolic volume (LVES), left ventricular end-diastolic diameters (LVED) and posterior wall end-diastolic thickness (LVPW) were recorded from the LV M-mode tracing with a sweep speed of 50 mm/s at the mid-papillary muscle level. The percentage of fractional shortening (FS%) was calculated as (LVED-LVES)/LVED × 100%.

2.2. H&E staining

The hearts were excised, rinsed with PBS, arrested in diastolic phase with 10% potassium chloride solution, weighed, placed in 10% formalin, and embedded in paraffin. They were then cut transversely and near the apex to image the left and right ventricles. Different parts of each heart (4–5 mm thick) were used to stain with hematoxylin and eosin (H&E) (Beyotime, China) for histopathological examination using standard procedures and then observed with an optical microscope (Olympus, Japan).

2.3. Cell morphological analysis

H9c2 rat cardiomyocyte cells (ATCC, Rockville, MD, USA) were cultured as described previously [25]. H9c2 cells were plated at a density of 1×10^6 cells/well onto 6-well plates in a mixture of Dulbecco's modified Eagle's medium (DMEM) and F12 medium at a ratio of 1:1 (v/v) with 10% fetal bovine serum (FBS) (GBICO, USA), glutamine (2 mmol/L), penicillin (100 IU/mL), and streptomycin (100 mg/mL) (Beyotime, China). After 48 h, we replaced the culture medium with F10 medium containing 0.1% FBS (GBICO), and treated the cells with angiotensin II (Ang II; 1 μM for 48 h) (Sigma, USA). To visualize cellular membranes, FITC-WGA (ThermoFisher, USA) was used. For nucleus staining, DAPI (Sigma) was applied. All the images were captured using a camera mounted on an inverted microscope (Olympus).

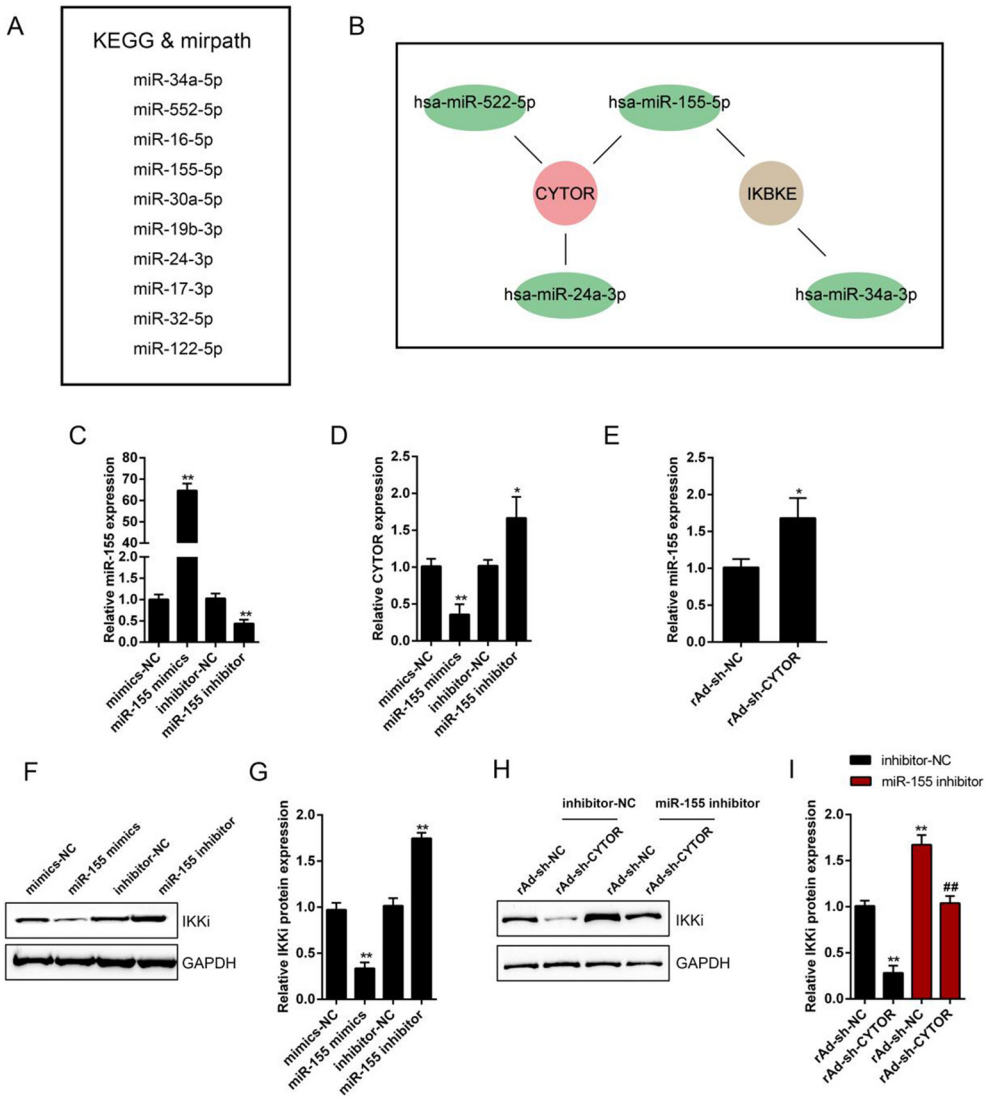

Fig. 4. CYTOR modulates IKKi through miR-155 (A) A total of 10 miRNAs related to Hypertrophic cardiomyopathy (HCM, hsa05410) annotated by KEGG and mirpath signaling pathway analyses. (B) ceRNA network constructed by Targetscan consists of CYTOR, IKBKE and miRNAs. (C) miR-155 expression was achieved by transfection of miR-155 mimics or miR-155 inhibitor, as confirmed using real-time PCR. (D) CYTOR expression in response to miR-155 overexpression or miR-155 inhibition examined using real-time PCR. (E) miR-155 expression in response to CYTOR knockdown examined using real-time PCR. (F–G) Myocytes were transfected with miR-155 mimics or miR-155 inhibitor and examined for the protein levels of IKKi using Immunoblotting. (H–I) Myocytes were co-transfected with si-CYTOR and miR-155 inhibitor and examined for the protein levels of IKKi using Immunoblotting. The data are presented as mean ± SD of three independent experiments. $*P < 0.05$, $**P < 0.01$, *vs.* mimics NC or inhibitor NC group; $\#\#P < 0.01$, *vs.* si-CYTOR group.

2.4. Cell transfection and infection

MiR-155 mimics, miR-155 inhibitor, mimics-NC and inhibitor-NC, were purchased from GenePharma (China) and transfected into target cells using Lipofectamine 2000 (Invitrogen, USA) according to the manufacturer's instructions. The H9c2 cells were infected with the rAd-sh-CYTOR or sh-NC at a multiplicity of infection (MOI) of 10 plaque forming units (PFU) per cell. Cells were harvested 48 h later after infection.

2.5. Real-time PCR

Total RNA was extracted with TRIzol reagent (Invitrogen) following the operating manual. With miRNA-specific primers, total RNA was reverse transcribed, and the miScript Reverse Transcription kit (Qiagen, Germany) was applied for miRNA qRT-PCR. The expression of RNU6B was used as an endogenous control. The SYBR green PCR Master Mix (Qiagen) was used for mRNA detection following the operating manual. The expression of GAPDH was used as an endogenous control. The ΔΔCT values indicated the relative fold changes.

2.6. Immunoblotting assays

First, RIPA buffer (Sigma) with a Complete Protease Inhibitor Cocktail (Roche, USA) was used to lyse cells, and cell lysates were transferred to 1.5 mL tubes and stored at −20 °C until use. Next, proteins were loaded onto an SDS-PAGE minigel and later transferred onto PVDF membranes (Beyotime, China). Third, we incubated the membranes with the following antibodies at 4 °C overnight: anti-ANP (PA3-228, Invitrogen), anti-BNP (MA1-91673, Invitrogen), anti-β-MHC (ab170867, Abcam, Cambridge, CA, USA), anti-IKKi (ab7891, Abcam), anti-p-NF-κB (Cat# 4228, CST, Danvers, MA, USA), anti-NF-κB (Cat# 4257, CST), anti-p-AKT (Cat# 4060, CST), anti-AKT (Cat# 4691, CST) and anti-GAPDH (ab8245, Abcam) and incubated with HRP-conjugated secondary antibody (1:5000). Finally, we visualize the protein signals using ECL Substrates (Millipore, USA). ImageJ software (NIH) was used to evaluate the gray intensity.

2.7. Luciferase reporter assay

For miR-155 binding to CYTOR (in rat named LOC100910286) or IKBKE, the fragment of CYTOR or IKBKE was amplified by PCR and cloned into the downstream region of the renilla psiCHECK2 plasmid (Promega, Madison, WI, USA), named wt-CYTOR or wt-IKBKE 3′UTR. To generate the CYTOR or IKBKE 3′UTR mutant plasmid, we mutated the seed region of the CYTOR or IKBKE 3′UTR to eliminate the complementary region to miR-155, and named mut-CYTOR or mut-IKBKE 3′UTR. HEK293 cells (ATCC, USA) were cultured in a 24-well plate.

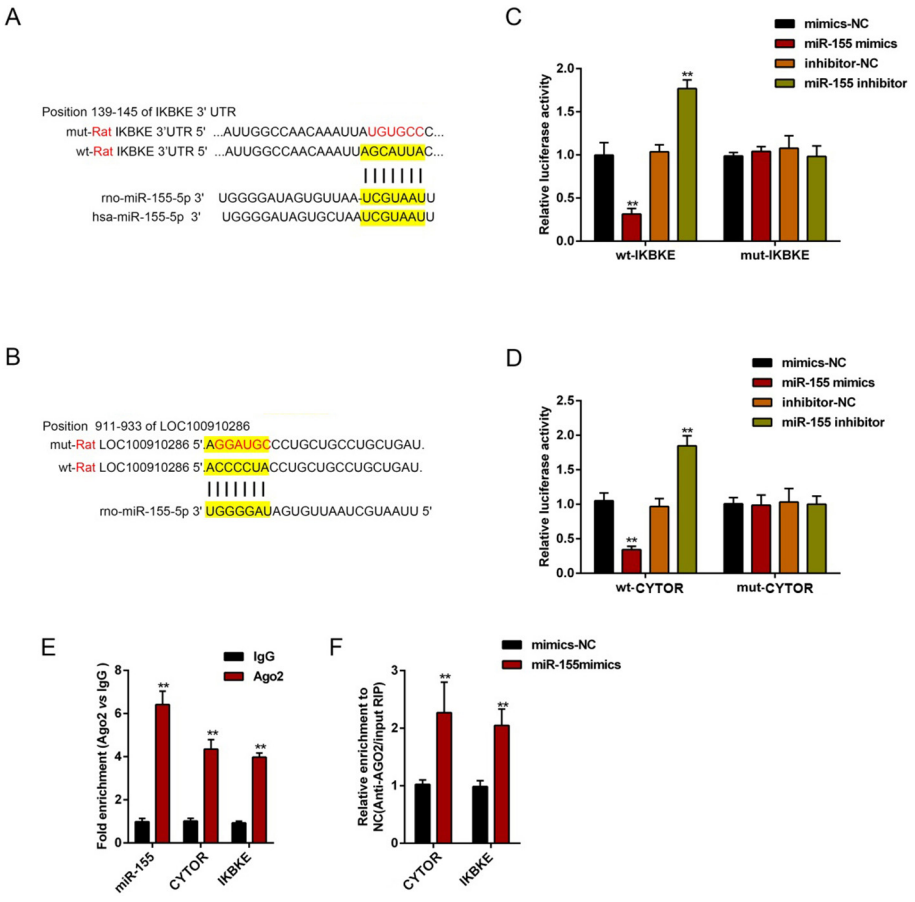

Fig. 5. CYTOR serves as a ceRNA for miR-155 to counteract miR-155-mediated repression of IKBKE (A–B) Wild-type and mutant-type IKBKE 3′UTR and CYTOR (in rat named LOC100910286) vectors were constructed and named wt-IKBKE 3′UTR, wt-CYTOR, mut-IKBKE 3′UTR and mut-CYTOR. Wild-type and mutant-type IKBKE 3′UTR and CYTOR vectors contained wild-type or mutated putative miR-155 binding site, respectively. (C–D) The above described vectors were co-transfected into HEK293 cells with miR-155 mimics or miR-155 inhibitor and examined for luciferase activity. (E–F) Association of miR-155, CYTOR and IKBKE with AGO2 in myocytes. Detection of AGO2 and IgG using Immunoblotting and detection of miR-155, CYTOR and IKBKE using real-time PCR. The data are presented as mean ± SD of three independent experiments. $^{*}P < 0.05$, $^{**}P < 0.01$.

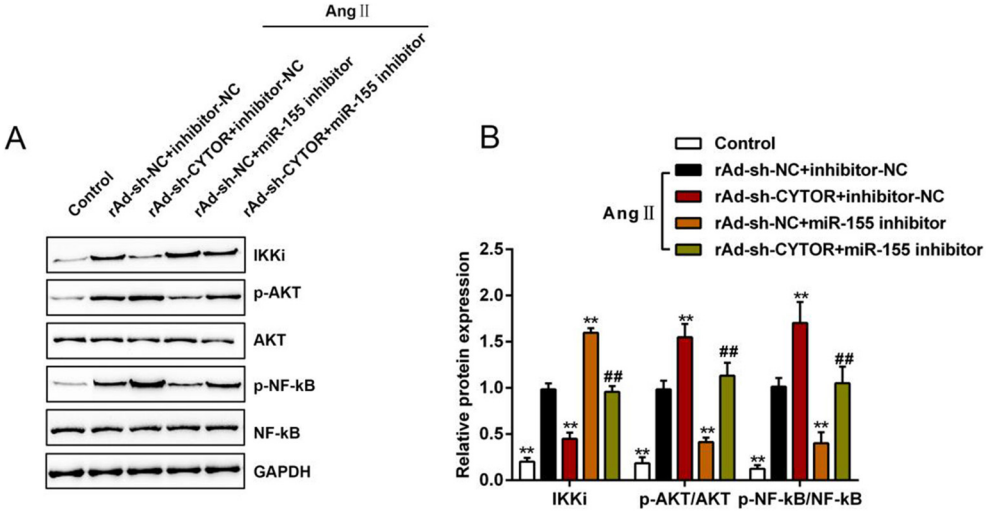

Fig. 6. CYTOR/miR-155 axis modulates Ang II-induced cardiomyocyte hypertrophy through IKKi signaling (A-B) Myocytes were co-transfected with si-CYTOR and miR-155 inhibitor and examined for protein levels of IKKi, p-NF-κB, NF-κB, p-AKT and AKT. The data are presented as mean ± SD of three independent experiments. $^{**}P < 0.01$, *vs.* si-NC + inhibitor-NC group in the presence of Ang II; $\#\#P < 0.01$, *vs.* si-CYTOR + inhibitor-NC group in the presence of Ang II.

After culturing overnight, HEK293 cells were co-transfected with the indicated vectors and miR-155 mimics or miR-155 inhibitor, respectively. After transfection for 48 h, luciferase assays were assessed with the Dual-Luciferase Reporter Assay System (Promega). The firefly luciferase activity of each transfected well was normalized to renilla luciferase activity.

2.8. RNA immunoprecipitation (RIP)

At first, we used a Magna RIP RNA-Binding Protein Immunoprecipitation Kit (17–700, Millipore) to precipitate RNA comply with the operating manual. Second, RNA was transcribed with a T7 High Yield RNA Synthesis Kit (E2040S, NEB, USA) also following the protocols. At last, we measured the levels of CYTOR, IKBKE, and miR-155 in immunoprecipitates by qRT-PCR.

2.9. Statistical analysis

Experimental data are processed with SPSS17.0 statistical software and presented as the average (mean ± S.D.) of results from at least three separate experiments. Student's *t*-test was used for statistical comparison where applicable. The above data with more than two groups were analyzed with one-way ANOVA. *P*-values < 0.05 were considered statistically different.

3. Results

3.1. Selection of differentially-expressed lncRNAs in cardiac hypertrophy

To identify differentially-expressed lncRNAs in the development of cardiac hypertrophy, we downloaded data from GEO database (GSE60291) and found that a total of 187 lncRNAs were dysregulated (fold-change > 4, $P < 0.001$) in human cardiac hypertrophy. Of them, lncRNA cytoskeleton regulator RNA (CYTOR), which was reported to be required in cytoskeleton organization in breast cancer cells [26], was significantly upregulated with a fold-change of 6.16 ($P < 0.01$, Fig. 1A). Moreover, based on the data from The Genotype-Tissue Expression (GTEx) project, CYTOR expression in the auricular and left ventricle was positively correlated with IKBKE, which has been reported to inhibit cardiac in our previous study [8] (Fig. 1B). Thus, CYTOR was selected for further experiments.

3.2. The effect of CYTOR knockdown on heart hypertrophy in vivo

To verify the effect of rAd-sh-CYTOR on CYTOR expression in mice hearts, the CYTOR expression was detected in rAd-sh-NC or rAd-sh-CYTOR-infected mice after sham or AB operation, respectively. 3 weeks after rAd-sh-CYTOR infection, CYTOR transcription was significantly reduced as compared to the rAd-sh-NC group (Fig. 2A). We also found that CYTOR transcription was markedly upregulated in AB group compared to that in the sham group (Fig. 2A).

The histological analysis confirmed the increase in ventricle wall thickness in CYTOR knockdown mice (rAd-sh-CYTOR-infected mice) in response to AB, whereas AB-induced hypertrophy was evident in ventricles of control mice (Fig. 2B). Anatomic and Echocardiography analyses were then performed to document cardiac structure and cardiac function changes four weeks after AB. AB operation significantly increased chamber wall thickness and led to cardiac dyfunction after pressure overload (Fig. 2C–F, $\#P < 0.05$). Moreover, CYTOR knockdown hearts partially lost ventricular systolic function under pressure overload, as evidenced by the substantially lower FS% in CYTOR knockdown mice in both sham and AB group as compared with control mice (rAd-sh-NC-infected mice) in sham and AB groups respectively (Fig. 2C). The ratio of heart weight to body weight (HW/BW), LVPW and LVES in CYTOR knockdown mice increased, particularly after AB operation, as compared to that of control mice (Fig. 2D–F). Next, we detected the marker protein of hypertrophy, ANP, BNP and β-MHC in the CYTOR knockdown and control mice after AB or sham operation. The ANP, BNP, β-MHC protein levels were remarkably upregulated in CYTOR knockdown mice, and further increased after AB operation as compared with the control mice (Fig. 2G–H). Together, these data demonstrate that CYTOR knockdown aggravated AB-induced cardiac hypertrophy.

3.3. CYTOR knockdown aggravates Ang II-induced cardiomyocyte hypertrophy in vitro

To explore the molecular mechanism, we transfected H9c2 cells with sh-CYTOR and then treated with Ang II (1 μM for 48 h). The transfection of sh-CYTOR significantly enlarged the cell size, which was further enlarged by Ang II treatment (Fig. 3A–B). Moreover, Immunoblotting revealed that CYTOR knockdown markedly increased the expression of ANP, BNP, and β-MHC, especially after Ang II treatment (Fig. 3C–D). These *in vitro* data suggest that CYTOR knockdown aggravates cardiomyocyte hypertrophy.

3.4. CYTOR modulates IKKi through miR-155

As we have mentioned, CYTOR expression was positively correlated with IKBKE, which could protect hearts from developing pathological cardiac hypertrophy [8]. Due to the critical roles of miRNAs in cardiac hypertrophy [27–29], KEGG and Mirpath signaling pathway analyses were performed to annotate miRNAs related to Hypertrophic cardiomyopathy (HCM, hsa05410) and a total of 10 most relevant miRNAs were identified (Fig. 4A). Next, Targetscan was used to construct a ceRNA network consist of CYTOR, IKBKE, and miRNAs; of involved miRNAs, miR-155 was predicted to target both CYTOR and IKBKE (Fig. 4B). The loss of miR-155 has been reported to prevent cardiac hypertrophy developing [23]; thus, we chose miR-155 for more in-depth experiments. To prove the predicted interaction between miR-155 and CYTOR and IKBKE, respectively, we achieved miR-155 expression in H9c2 cells by transfecting miR-155 mimics or miR-155 inhibitor, as confirmed using qPCR (Fig. 4C). CYTOR expression was negatively regulated by miR-155 (Fig. 4D), and miR-155 expression was upregulated by CYTOR knockdown (Fig. 4E). Moreover, the IKKi protein was negatively related to miR-155 (Fig. 4F–G). IKKi protein was decreased by CYTOR knockdown while increased by miR-155 inhibition; miR-155 inhibition could partially attenuate the effect of CYTOR knockdown (Fig. 4H–I). These data indicate that CYTOR may serve as a sponge for miR-155 to reduce miR-155-induced suppression of IKBKE.

3.5. CYTOR function as a "sponge" for miR-155 to reduce miR-155-induced suppression of IKBKE

After confirming the dynamic effect of CYTOR/miR-155 axis on IKBKE, the targeted binding of miR-155 to CYTOR and IKBKE, respectively, was validated using Immunoblotting and RIP assays. We constructed wild-type and mutant-type luciferase reporter plasmids, including wt-CYTOR, mut-CYTOR, wt-IKBKE 3′UTR and mut-IKBKE 3′UTR; wild-type plasmids contained predicted miR-155 binding site(s) while mutant-type plasmids contained any of the mutated miR-155 binding sites (Fig. 5A–B). These plasmids were co-transfected into HEK293 cells with miR-155 mimics or miR-155 inhibitors, respectively, and detected for luciferase activity. The luciferase activity of wild-type plasmids could be remarkably decreased by miR-155 mimics while increased by miR-155 inhibitors; after mutated the predicted miR-155 binding site(s), no changes in luciferase activity (Fig. 5C–D).

To confirm the bindings further, we employed RIP assays. As shown in Fig. 5E, miR-155, CYTOR, and IKBKE were associated with the AGO2 in HEK293 cells. In RNA extracted from precipitated AGO2 protein, the levels of miR-155, CYTOR, and IKBKE were dramatically higher than IgG. We also performed RIP assay in HEK293 cell line transfected with control miRNA (mimics-NC) or miR-155 mimics followed by real-time PCR to detect CYTOR and IKBKE associated with AGO2; the results shown in Fig. 4F confirmed the interaction between miR-155 and CYTOR, and between miR-155 and IKBKE.

3.6. CYTOR/miR-155 axis modulates Ang II-induced cardiomyocyte hypertrophy through IKKi signaling

Since CYTOR/miR-155 axis could regulate IKBKE, next, the dynamic effect of CYTOR/miR-155 axis on IKKi signaling was evaluated. We co-transfected si-CYTOR and miR-155 inhibitor into H9c2 cells and then examined the protein expression of IKKi, p-NF-κB, NF-κB, p-AKT, and AKT. As shown in Fig. 6A and B, CYTOR knockdown significantly reduced IKKi protein while increased the ratio of p-NF-κB/NF-κB and p-AKT/AKT; miR-155 repression played an opposing role on IKKi signaling; the impact of CYTOR downregulation could be partially attenuated by miR-155 suppression.

4. Discussion

In our current research, we revealed that lncRNA CYTOR expression was remarkably upregulated in cardiac and cardiomyocyte hypertrophy. CYTOR knockdown could aggravate AB-induced cardiac hypertrophy or Ang II-induced cardiomyocyte hypertrophy *in vitro* and *in vivo*. Moreover, by using KEGG and Mirpath signaling analyses, miRNAs

and ceRNA network related to hypertrophic cardiomyopathy (HCM, |hsa05410) were annotated, and miR-155 was predicted to target CYTOR and IKBKE. CYTOR function as a ceRNA for miR-155 to reduce miR-155-induced suppression of IKBKE. CYTOR/miR-155 axis modulated the downstream IKKi and NF-κB signaling pathways.

There is growing evidence showed that lncRNAs regulate heart hypertrophy. Cardiac hypertrophy-associated epigenetic regulator (Chaer) interacts directly with polycomb repressor complex 2 (PRC2) to suppress the histone H3 lysine 27 methylation in the promoter regions of the gene involved in cardiac hypertrophy, thereby promoting cardiac hypertrophy [18]. Cardiac hypertrophy-associated transcript (Chast) is another pro-hypertrophy lncRNA, which is increased in hypertrophic hearts, inhibits CM autophagy and induces hypertrophy by negatively regulating Plekhm1 [30]. Cardiac hypertrophy-related factor (CHRF) is increased in both the hypertrophic mouse heart and human heart failure specimens [20]. In the present study, we analyzed a microarray result from GEO database (GSE60291) and found CYTOR expression was markedly increased in cardiac hypertrophy. More importantly, its expression was positively correlated with IKBKE in the auricular and the left ventricle. In our previous study, we revealed that IKBKE could protect hearts from developing pathological cardiac hypertrophy through IKKi and NF-κB signaling [8]. Here, CYTOR expression was significantly upregulated in AB-induced cardiac hypertrophy, which was consistent with the indicated microarray analysis results. Moreover, CYTOR knockdown aggravated AB operation-induced cardiac hypertrophy *in vivo* and Ang II-induced cardiomyocyte hypertrophy *in vitro*, suggesting that CYTOR may protect hearts from cardiac hypertrophy.

Regarding the molecular mechanism, lncRNAs may act as an endogenous 'sponge' to inhibit the function of miRNAs, which induce translational repression of downstream targets [22]. As above mentioned, CHRF promotes cardiac hypertrophy by downregulating the expression of anti-hypertrophy miRNA, miR-489, which target gene is Myd88. Meanwhile, Myd88 could activate the NF-κB pathway [20]. Since we have stated the protective role of IKBKE in cardiac hypertrophy [8] and the positive correlation between CYTOR and IKBKE, here, we performed KEGG and Mirpath annotation to construct a ceRNA network consist of CYTOR, IKBKE, and miRNAs. Of involved miRNAs, miR-155 was predicted to target both CYTOR and IKBKE. Interestingly, miR-155 itself has a crucial effect in heart hypertrophy. Contrary to CYTOR, miR-155 loss plays a beneficial role in heart hypertrophy [23]. Here, we observed a negative dual-regulation between CYTOR and miR-155; more importantly, CYTOR could promote the protein level of IKKi in myocytes through miR-155, suggesting that CYTOR may serve as a ceRNA for miR-155 to reduce miR-155-induced suppression of IKBKE.

To validate this hypothesis, we further verified the targeted binding sites of miR-155 to CYTOR and IKBKE. As expected, miR-155 targeted both CYTOR and IKBKE through direct binding. More importantly, CYTOR knockdown induced the activation of IKKi and NF-κB signaling, which was consistent with our previous study that IKKi deficiency-induced cardiac hypertrophy is associated with the activation of the AKT and NF-κB signaling pathway in response to AB operation [8]. miR-155 inhibition exerted an opposing effect on IKKi and NF-κB signaling, and partially attenuated the effect of CYTOR knockdown, indicating that CYTOR may modulate cardiac hypertrophy through miR-155 and downstream IKKi and NF-κB signaling.

Taken together, CYTOR may present a protective effect in cardiac hypertrophy through regulating miR-155 and downstream IKKi and NF-κB signaling pathways, most likely *via* the mechanism that CYTOR functions as a ceRNA for miR-155 to reduce miR-155-induced suppression of IKBKE, thus affecting downstream IKKi and NF-κB signaling.

Sources of funding

This work was supported by the National Natural Science Foundation of China (no. 81660039, 81700218), Natural Science Foundation of Hubei Province, China (no. 2017CFB320).

Disclosures

None.

Transparency document

The Transparency document associated with this article can be found, in online version.

References

[1] J. Veselka, N.S. Anavekar, P. Charron, Hypertrophic obstructive cardiomyopathy, Lancet 389 (10075) (2017) 1253–1267.
[2] T. Stanton, F.G. Dunn, Hypertension, left ventricular hypertrophy, and myocardial ischemia, Med. Clin. North Am. 101 (1) (2017) 29–41.
[3] L. Schirone, et al., A review of the molecular mechanisms underlying the development and progression of cardiac remodeling, Oxidative Med. Cell. Longev. 2017 (2017) 3920195.
[4] B.C. Bernardo, et al., Molecular distinction between physiological and pathological cardiac hypertrophy: experimental findings and therapeutic strategies, Pharmacol. Ther. 128 (1) (2010) 191–227.
[5] Diwan, A. and G.W. Dorn, 2nd, Decompensation of cardiac hypertrophy: cellular mechanisms and novel therapeutic targets. Physiology (Bethesda), 2007. 22: p. 56–64.
[6] T. Matsui, A. Rosenzweig, Convergent signal transduction pathways controlling cardiomyocyte survival and function: the role of PI 3-kinase and Akt, J. Mol. Cell. Cardiol. 38 (1) (2005) 63–71.
[7] J.P. Guo, D. Coppola, J.Q. Cheng, IKBKE protein activates Akt independent of phosphatidylinositol 3-kinase/PDK1/mTORC2 and the pleckstrin homology domain to sustain malignant transformation, J. Biol. Chem. 286 (43) (2011) 37389–37398.
[8] J. Dai, et al., IKKi deficiency promotes pressure overload-induced cardiac hypertrophy and fibrosis, PLoS One 8 (1) (2013) e53412.
[9] E.P. Consortium, An integrated encyclopedia of DNA elements in the human genome, Nature 489 (7414) (2012) 57–74.
[10] A. Jandura, H.M. Krause, The new RNA world: growing evidence for long noncoding RNA functionality, Trends Genet. 33 (10) (2017) 665–676.
[11] M. Klingenberg, et al., Non-coding RNA in hepatocellular carcinoma: mechanisms, biomarkers and therapeutic targets, J. Hepatol. 67 (3) (2017) 603–618.
[12] M. Esteller, Non-coding RNAs in human disease, Nat. Rev. Genet. 12 (12) (2011) 861–874.
[13] T. Yang, et al., Cardiac hypertrophy and dysfunction induced by overexpression of miR-214 in vivo, J. Surg. Res. 192 (2) (2014) 317–325.
[14] I. Karakikes, et al., Therapeutic cardiac-targeted delivery of miR-1 reverses pressure overload-induced cardiac hypertrophy and attenuates pathological remodeling, J. Am. Heart Assoc. 2 (2) (2013) e000078.
[15] A. Care, et al., MicroRNA-133 controls cardiac hypertrophy, Nat. Med. 13 (5) (2007) 613–618.
[16] L. Lv, et al., The lncRNA Plscr4 controls cardiac hypertrophy by regulating miR-214, Mol. Ther.–Nucleic Acids 10 (C) (2018) 387–397.
[17] Micheletti, R., et al., The long noncoding RNA Wisper controls cardiac fibrosis and remodeling. Sci Transl Med, 2017. 9(395):eaai9118.
[18] Z. Wang, et al., The long noncoding RNA Chaer defines an epigenetic checkpoint in cardiac hypertrophy, Nat. Med. 22 (10) (2016) 1131–1139.
[19] Liu, L., et al., The H19 long noncoding RNA is a novel negative regulator of cardiomyocyte hypertrophy. Cardiovasc. Res., 2016. 111(1): p. 56–65.
[20] K. Wang, et al., The long noncoding RNA CHRF regulates cardiac hypertrophy by targeting miR-489, Circ. Res. 114 (9) (2014) 1377–1388.
[21] A.L. Sarver, S. Subramanian, Competing endogenous RNA database, Bioinformation 8 (15) (2012) 731–733.
[22] L. Salmena, et al., A ceRNA hypothesis: the Rosetta Stone of a hidden RNA language? Cell 146 (3) (2011) 353–358.
[23] H.Y. Seok, et al., Loss of MicroRNA-155 protects the heart from pathological cardiac hypertrophy, Circ. Res. 114 (10) (2014) 1585–1595.
[24] A.M. Feldman, et al., Selective changes in cardiac gene expression during compensated hypertrophy and the transition to cardiac decompensation in rats with chronic aortic banding, Circ. Res. 73 (1) (1993) 184–192.
[25] N. Sambandam, et al., Malonyl-CoA decarboxylase (MCD) is differentially regulated in subcellular compartments by 5'AMP-activated protein kinase (AMPK). Studies using H9c2 cells overexpressing MCD and AMPK by adenoviral gene transfer technique, Eur. J. Biochem. 271 (13) (2004) 2831–2840.
[26] O. Van Grembergen, et al., Portraying breast cancers with long noncoding RNAs, Sci. Adv. 2 (9) (2016) e1600220.
[27] M. Tatsuguchi, et al., Expression of microRNAs is dynamically regulated during cardiomyocyte hypertrophy, J. Mol. Cell. Cardiol. 42 (6) (2007) 1137–1141.
[28] C. Bang, et al., Cardiac fibroblast-derived microRNA passenger strand-enriched exosomes mediate cardiomyocyte hypertrophy, J. Clin. Invest. 124 (5) (2014) 2136–2146.
[29] E. Shen, et al., MicroRNAs involved in the mitogen-activated protein kinase cascades pathway during glucose-induced cardiomyocyte hypertrophy, Am. J. Pathol. 179 (2) (2011) 639–650.
[30] Viereck, J., et al., Long noncoding RNA Chast promotes cardiac remodeling. Sci Transl Med, 2016. 8(326): p. 326ra22.